



Numerical study of cuttings transport of nanoparticle-based drilling fluid

Mortatha Al-Yasiri^{1,2} | Amthal Al-Gailani³ | Dongsheng Wen^{3,4}

¹Al-Amarah University College, Misan, Iraq

²College of Engineering, University of Misan, Misan, Iraq

³University of Leeds, Leeds, UK

⁴Beihang University, Beijing, China

Correspondence

Mortatha Al-Yasiri, Al-Amarah University College, Misan, Iraq.

Email: mortathasaadon@gmail.com

Abstract

Cuttings transportation from the drill bit, through the annulus, to the surface is one of the most important functions performed by drilling fluid. The prediction of drilling fluid's performance to transport cuttings in the annulus is very complex task due to the presence of numerous parameters. Nanoparticles (NPs) have been recently introduced into drilling fluid to engineer its properties and enhance its performance. Nevertheless, the lifting capacity has not been sufficiently investigated. The understanding of the influence and the mechanisms responsible for the improvement in cuttings transport process can further advance the application of NPs for drilling fluids. Computational fluid dynamics (CFD) is widely used as a numerical technique in handling complex multiphase flow problems in different operational conditions. The present work has taken the advantages of CFD to computationally analyze the influence of NPs and the effects of various parameters such as drilling fluids rheology, flow rate, pipe rotation, cuttings density, shape, concentration, and drilling fluids-cuttings particle coupling regimes on the cuttings transport in a vertical wellbore. The CFD simulation is carried out by using transient solver of ANSYS-FLUENT commercial code. The dense discrete phase model is used to overcome the main shortcomings of previous Eulerian based approaches. Good agreement has been achieved between the simulation and the published experimental results. It showed that the fluid viscosity and cuttings transport process can be significantly enhanced by adding nanomaterials to the fluid, and the process is highly influenced by cuttings characteristics such as in situ concentration, shape, and density.

KEYWORDS

CFD, cuttings transport, drilling fluids, multiphase flow, nanoparticles, rheology, wellbore

Abbreviations: CFD, computational fluid dynamics; DDPM, dense discrete phase model; DEM, discrete element method; HTHP, high temperature and high pressure; LTLP, low temperature and low pressure; NPs, nanoparticles; OBM, oil-based mud; RANS, Reynolds-averaged Navies-Stokes; UDF, user-defined function; WBM, water-based mud.

This is an open access article under the terms of the Creative Commons Attribution License, which permits use, distribution and reproduction in any medium, provided the original work is properly cited.

© 2020 The Authors. *Engineering Reports* published by John Wiley & Sons, Ltd.

1 | INTRODUCTION

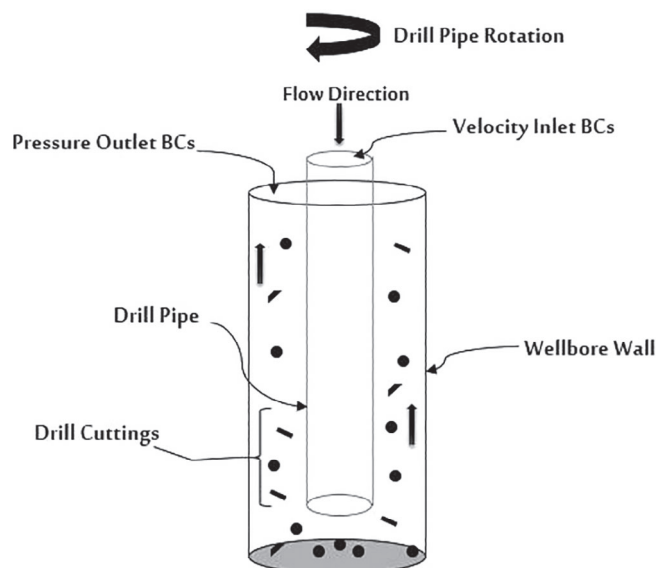
The drilling fluids perform many functions such as cooling and transporting cuttings from the bottom to the surface. Wellbore cleaning is an important task of drilling fluids and it should be well performed in drilling operations to avoid problems such as stick pipe, high torque and drag and loss circulation. Nanomaterials have been recently introduced as additives to improve drilling fluids performance and to meet the operational, technical, and environmental requirements.^{1,2} It enhances the drilling fluids rheological properties, filter cake quality, and carrying capacity. The concentration of nanoparticles (NPs) plays an important role in improving the fluid performance.³ Most of the reported studies investigated the influence of NPs on the laboratory benches using a rheometer and filtration setup.⁴⁻⁶

The influence of nanomaterials on the characteristics and performance of drilling fluids has been experimentally studied at different conditions.⁷⁻¹⁵ However, the laboratory investigations do not always reflect the fluid behavior and properties that flowing through circulation system under various conditions. Computational fluid dynamics (CFD) is an analysis method, which analyzes fluid flow, heat, and mass transfer, and other phenomena in different regimes.¹⁶ Using CFD technique for investigating the drilling fluid flow and rheology in wellbore could reduce experiment cost and time, producing unlimited data. Inefficient removal of cuttings would increase the cutting accumulation and lead to mechanical pipe sticking, impeding the drilling process.¹⁷ Therefore, it is important to simulate and understand the influence of various parameters such as drilling fluids rheology, flow rate, pipe rotation, cuttings density, shape, and concentration on the cuttings transport.

There are many investigations of nanomaterials influence on the thermal stability and rheology of drilling mud reported in the literature.^{18,19} Laponite NPs have been used to improve the onset decomposition temperature of and viscosity of the polymer in the drilling fluids at high-temperature and high-pressure conditions.²⁰ The study findings show that the viscosity of drilling fluids with laponite NPs had a higher decomposition point and greater viscosity than those without laponite NPs. The thermal stability and the rheological properties of drilling fluids have been also enhanced using nanosized layered particles. The rheological tests for drilling fluids containing magnesium aluminum silicate NPs indicated that the shear-thinning performance, carrying capacity, and gel strength have been significantly improved when compared with base drilling fluids.²¹ In addition to the thermal stability, the thermal conductivity is also important property in cooling function of drilling fluids. Saboori et al²² reported that copper oxide NPs enhanced the thermal conductivity by 29% and reduced the temperature gradient about twice when compared to the base fluids.

The cuttings-drilling fluids flow can be simulated as solid-liquid flow, with the cutting as solid particles while the drilling fluid as non-Newtonian fluid. The literature on cuttings transportation shows a variety of modeling approaches. The choosing of the suitable model is a real serious concern. Drilling fluid-cuttings flow modeling is a complicated task, but it is a really useful tool to infer more about these flows. Several researchers have proposed to use Eulerian-Eulerian approach to model drilling fluids-cuttings flow.^{23,24} This strategy usually requires much less computational resources corresponded to Eulerian-Lagrangian schemes. Thus, it can be employed to model pilot scale.^{25,26} However, the discrete nature of the solid phase is missing in the Eulerian-Eulerian strategy due to the continuous representation of the dispersed phase. This weakness can be surmounted with the discrete element method (DEM).²⁷⁻²⁹ In this approach, the solid particles are tracked separately based on Newton's laws of motion besides particle-particle and particle-wall collisions. Not only Eulerian approach has limitations but also the Lagrangian approach. One of the main shortcomings of DEM technique is the high computational demands that reduce its applications to small scale.³⁰ Discrete phase model was used in the simulation of cuttings to eliminate the previous restrictions,³¹ which is two-ways coupling between the cuttings and fluid. As a result of using DPM, the volume fraction of the discrete phase should not be exceeded 10%, otherwise weak accurate predictions will be obtained. To avert all previous approaches limitation, the dense discrete phase model (DDPM) has been established in which the details of particle-particle and particle-wall collisions are not overtly tracked anymore; as an alternative, a force is employed to represent these collisions.³² Moreover, the hypothesis of the particles bundle is utilized to lessen the amounts of particles included in the computations, resulting in an important acceleration of the speed of the calculations. Therefore, the DDPM looks promising considering to the advantages of Lagrangian methods and is applicable to large scales.

The DDPM model is suggested in this work to overcome the main shortcomings of Eulerian-Eulerian and CFD-DEM approaches. DDPM has the powers of easy implementation of realistic particle size distribution and tracking the discrete character of particles. It is also less computational cost than Eulerian-Eulerian approach,³³ since the coarse grid can be employed to perform grid-size-independent simulations and the application of the idea of the bundle.

FIGURE 1 Problem configuration**TABLE 1** Meshes size and characteristics

Mesh	Cells	Faces	Nodes	Cell zone	Face zones	Max aspect ratio	Min orthogonal quality
Coarse	77 520	237 460	82 477	1	7	34.8	0.7
Medium	127 182	388 003	133 712	1	7	23	0.715
Fine	172 250	525 239	180 820	1	7	20.8	0.716

Although several studies have been conducted in recent years, no attention has been paid to the effect of cuttings concentration as well as the effects of NPs on drilling fluids properties. To address this gap, this work proposes to numerically investigate the effects of drilling fluids flow, cuttings transport, and NPs. The first objective of the study is to simulate the flow behavior of the suspended cuttings in a non-Newtonian NP-based drilling fluid. Secondly, a parametric study of the cuttings transport process, including fluid flow rate, cuttings shape, density and in situ concentration is performed. Finally, the analysis of NP influence on the fluid viscosity and the hole cleaning efficiency is conducted.

2 | METHODOLOGY

2.1 | Geometry, meshing, and boundary conditions

The 3D geometry consists of two overlapped cylindrical bodies (Figure 1). The interior cylinder represents a concentric rotating carbon steel drill pipe with an outer diameter of 0.05 m and a length of 1 m. The outer cylinder is a vertical and stationary wellbore with an inner diameter of 0.1 m and length of 1.2 m. To simplify the calculations, the model adopted here is based on the following assumptions: (a) wellbore formation is not a porous media; (b) the investigations have been applied to a specific section of whole drill pipe; (c) the drill bit has not been considered in the oil drilling system; and (d) the construction material wellbore is the Basalt rock which widely exists in the continental crust layer.

The geometry was created by Design Modeler/ANSYS. The unstructured mesh of hexahedral cells and quadrilateral faces was generated using ICEM CFD v.15. The dependency of the mesh size was eliminated by creating three different size meshes, and the medium one was selected for further simulations, as displayed in Table 1. The simulations were implemented on two computers. The first computer consists of Intel Core i5-3210M CPU @ 2.5 GHz and 4 GB of RAM, and the second one is the High-Performance Computer (HPC)/ARC2 at the University of Leeds which contains 380 CPUs.

2.2 | Mathematical formulations

The simulation of this system adopts a time-dependent model for fluid flow and concentration profiles in the oil drilling system. The incompressible, non-Newtonian, turbulent, multiphase flow of drilling fluids/particles has been mimicked in a three-dimensional (3D), transient CFD simulations using ANSYS-FLUENT. Among the different rheological models suggested for non-Newtonian drilling fluids, the Herschel-Bulkley model was used. For turbulence modeling, the standard k - ϵ turbulence model was used.

The flow field of the dispersed phase (particles) and continuum fluid phase has been calculated based on Eulerian-Lagrangian approach. The dispersed phases represent two groups of the suspended particulates, namely drilled cuttings and NPs. The discrete phase and continuum phase have been coupled via two-way coupling regime (DDPM). The forces included for reinforcing the fluid-particles interactions were drag force, pressure gradient force, lift force and two-way turbulence coupling. The inclusion of two-way turbulence coupling model was to determine the motion of the particles due to the flow turbulence. NP material and quantity were adopted from the experimental work of Alyasiri et al³⁴ (graphite and aluminum oxide with total concentrations of 0.3 and 0.9 wt%, respectively).

The energy equation was activated in the simulations for examining the effects of the wellbore wall temperature on the fluid rheology. The heat flux from the wellbore bottom was constant for maintaining the wall temperature around 360 K. The heat flux from wall linearly increases with the well depth, which was modeled using a user-defined function (UDF). The governing equations of flow for the discrete and continuous phases are displayed as follows:

2.2.1 | Continuous phase

The 3D momentum and mass conservation equations for incompressible, transient and viscous fluid flow are characterized by the local Reynolds-averaged Navier-Stokes (RANS) equations,^{16,35,36} as follows:

Mass conservation equation:

$$\frac{\partial}{\partial t}(\alpha_q \rho_q) + \nabla \cdot (\alpha_q \rho_q \vec{v}_q) = \sum_{p=1}^n (\dot{m}_{pq} - \dot{m}_{qp}) + S_q \quad (2.1)$$

Momentum conservation equation:

$$\begin{aligned} \frac{\partial}{\partial t}(\alpha_q \rho_q \vec{v}_q) + \nabla \cdot (\alpha_q \rho_q \vec{v}_q \vec{v}_q) = & -\alpha_q \nabla p + \nabla \cdot \bar{\tau}_q + \alpha_q \rho \vec{g} + \sum_{p=1}^n (\vec{R}_{pq} + \vec{v}_{qp} \dot{m}_{pq} - \vec{v}_{qp} \dot{m}_{qp}) \\ & + (\vec{F}_q + \vec{F}_{lift,q} + \vec{F}_{wt,q} + \vec{F}_{vm,q} + \vec{F}_{td,q}) \end{aligned} \quad (2.2)$$

The transport equations for the standard k - ϵ turbulence model are shown below³⁷:

$$\frac{\partial}{\partial t}(\rho k) + \frac{\partial}{\partial x_i}(\rho k v_i) = \frac{\partial}{\partial x_j} \left[\left(\mu + \frac{\mu_t}{\sigma_k} \right) \frac{\partial k}{\partial x_j} \right] + G_k + G_b - \rho \epsilon - Y_M + S_k \quad (2.3)$$

$$\frac{\partial}{\partial t}(\rho \epsilon) + \frac{\partial}{\partial x_i}(\rho \epsilon v_i) = \frac{\partial}{\partial x_j} \left[\left(\mu + \frac{\mu_t}{\sigma_\epsilon} \right) \frac{\partial \epsilon}{\partial x_j} \right] + C_{1\epsilon} \frac{\epsilon}{k} (G_k + C_{3\epsilon} G_b) - C_{2\epsilon} \rho \frac{\epsilon^2}{k} + S_\epsilon \quad (2.4)$$

The energy conservation in the Eulerian multiphase flow model is described by the independent steady-state enthalpy, as written below for each phase:

$$\frac{\partial}{\partial t}(\alpha_q \rho_q h_q) + \nabla \cdot (\alpha_q \rho_q \vec{u}_q h_q) = \alpha_q \frac{\partial p_q}{\partial t} + \bar{\tau}_q : \nabla \vec{u}_q - \vec{q}_q + S_q + \sum_{p=1}^n (Q_{pq} + m_{pq} h_{pq} - m_{qp} h_{qp}) \quad (2.5)$$

Fluid non-Newtonian behavior is addressed using the Herschel-Bulkley model. The governing equation the model is described:

$$\eta = \frac{\tau_0}{\gamma} + \kappa \left(\frac{\gamma}{\gamma_c} \right)^{n-1} \quad (2.6)$$

2.2.2 | Discrete phase

Using the Lagrangian approach, FLUENT predicts the trajectory of particles by integrating the force balance on the particles. The force balance equates the particle inertia with forces applying on particles like drag force, gravity force, rotational lift force, and so on.^{36,38,39} The equation of particle force balance can be written as follows:

$$\frac{d\vec{u}_p}{dt} = F_D(\vec{u} - \vec{u}_p) + \frac{(\rho_p - \rho)\vec{g}}{\rho_p} + \vec{F} \quad (2.7)$$

where \vec{F} refers to forces term that may include different possible forces such as gravity force, Saffman's lift force, pressure gradient force, and so on depending on the configurations. The drag force per unit particle mass F_D is described as

$$F_D = \frac{18\mu}{\rho_p d_p^2} \frac{C_D Re}{24} \quad (2.8)$$

The pressure gradient in the fluid:

$$\vec{F} = \frac{\rho}{\rho_p} u_p \nabla u \quad (2.9)$$

And particle lift due to shear, which is also known as Saffman's lift force⁴⁰:

$$\vec{F} = \frac{2Kv^{\frac{1}{2}} \rho d_{ij}}{\rho_p d_p (d_{kl} d_{lk})} (\vec{u} - \vec{u}_p) \quad (2.10)$$

The equations of volume fraction for each phase are individually solved using the implicit time discretization^{36,41,42} as written below:

$$V_q = \int_V \alpha_q dV \quad (2.11)$$

where

$$\sum_{q=1}^n \alpha_q = 1 \quad (2.12)$$

The boundary conditions for the base case include velocity inlet with fluid velocity magnitude of 10 m/s and pressure outlet for fluid/particles outlet. Cuttings particles are injected from the wellbore bottom with a size distribution modeled using the Rosin-Rammler method. The NPs are injected from the inlet of the drill pipe. The time step size for a transient solver for satisfactory convergence for fluid and particle phases is chosen as 0.001 second. Physical parameters of cuttings particles and NPs are listed in Tables 2 and 3, respectively.

3 | RESULTS AND DISCUSSION

3.1 | Model validation and mesh refinement study

3.1.1 | Model validation

The CFD model developed in this study is validated by experimental findings of Samsuri and Hamzah⁴³ work. They studied the effect of multiwalled carbon nanotubes (MWNTs) additive on the carrying capacity of drilling mud in a vertical well. MWNTs were added with different concentrations for various flow rates for investigating the mud lifting performance. To validate the model results, 0 and 0.01 wt % of NPs were simulated at flow velocity ranges from 0.05 to 0.15 m/s and compared with the experimental data. The orthorhombic cuttings particles were injected from the bottom of a well with a fixed size of 4.8 mm. As shown in Figure 2, a good agreement was obtained between the simulation results, especially at higher mud flow rates.

Property	Values
Max. diameter, m	0.005
Min. diameter, m	10^{-6}
Mean diameter, m	0.0025
Spread parameter	3
Particle density, kg/m^3	2300
Mass flow rate, kg/s	0.4
Particle volume, m^3	5.24×10^{-10} to 5.23×10^{-19}
Particle weight, g	1.95–0.0019
Temperature, K	300
X-velocity, m/s	0
Y-velocity, m/s	0.008

TABLE 2 Cuttings particle properties

Particles	Properties	Value
Graphite	Size, nm	50
	Shape	Spherical
	Density, kg/m^3	1800
	Thermal conductivity, w/m K	6
Aluminum oxide	Size, nm	45
	Shape	Spherical
	Density, kg/m^3	3500
	Specific heat, J/kg K	502.48
	Thermal conductivity, w/m K	202.4

TABLE 3 Nanoparticles physical properties

3.1.2 | Mesh refinement study

Three different sizes of meshes have been used to check the dependency on the mesh size, as presented in Table 1. Figure 3 displays a good agreement between the grids in term of velocity magnitude, turbulent kinetic energy (k), wall shear stress, and turbulence intensity. The refined medium grid has been selected for the further simulation to make a balance between the computational time and the accuracy of the predictions. The final mesh is an unstructured mesh of hexahedral cells and quadrilateral faces, as illustrated in Figure 3. Versteeg and Malalasekera¹⁶ reported that the optimal mesh should be non-uniform and fine in zones of high flow variation, and coarse in zones with low flow change. Hexahedral mesh offers excellent accuracy for RANS calculations at high Reynolds number and high viscous flow regions.⁴⁴ Good agreement between the grids results can be noticed from Figure 3D. This indicates that mesh size has no significant impact on the flow predictions.

3.2 | Fluid flow

The flow pattern of water-based drilling fluids through a rotating drill pipe and a wellbore has been investigated. Figure 4 reveals the streamlines and flow direction in the flow domain. Recirculation zones are formed near the corners of the wellbore bottom due to the great Reynolds number and sudden expansion in the flow area. The turbulent eddies in these zones could results in a loss of fluid, loss of heat and pressure drop.⁴⁵ The contour of fluid velocity shows a variation in the velocity components, as shown in Figure 4. The effects of drill pipe rotation on the fluid viscosity have been analyzed (Figure 5). The dynamic viscosity decreases with the share rate increase due to the non-Newtonian properties of the fluid.⁷

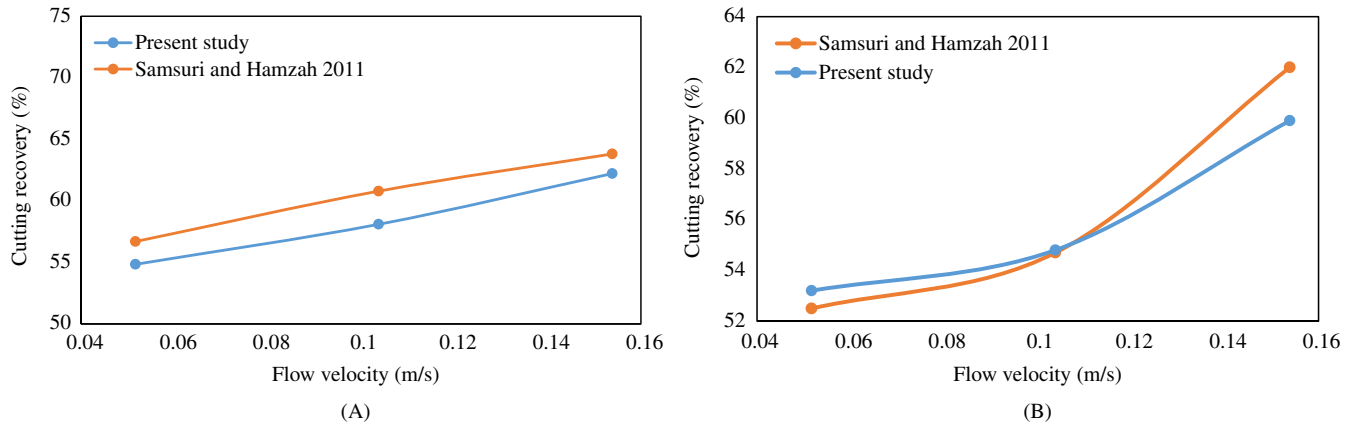


FIGURE 2 The experimental validation for the numerical findings of cuttings particle size 4.8 mm for, A, nanotreated fluid (0.01 wt% CNT NPs) and B, base fluid without NPs

The fluid viscosity contributes to the overall performance of drilling fluids in the hole cleaning process. The dynamic viscosity of non-Newtonian fluid has been studied with the variation of the shear rate and the NPs addition. The most critical parameter that affects the fluid viscosity is the drill pipe rotation speed (ie, shear rate). Figure 5 presents the effects of shear rate and NPs on the fluid viscosity. Adding nanomaterials in two concentrations promotes the fluid viscosity for different shear rates. NP concentration of 0.9 wt% shows a significant improvement in the viscosity, hence it has been considered for the cuttings transport investigations. The effective dispersion ability of NPs within the fluid structure could be the responsible for viscosity improvement.⁴⁶ Figure 6 depicts fluid viscosity distribution in the model through a cross-sectional view of the viscosity contour.

Figure 5 shows that the flow behavior of NP drilling fluid is similar to that of base fluid without NPs. Both drilling fluids with and without NPs followed the shear thinning behavior. The difference between them is that the addition of NPs renders higher viscosity, which is linked with the effective dispersion stability of NPs on the surface of bentonite.¹⁴

3.3 | Cuttings transport

The efficiency of nanofluid in the hole cleaning process was examined for different fluid flow rates and drilled cuttings characteristics. In the present model, the cuttings transport process was studied depending on the cuttings volume fraction in the outlet fluid. As described in the previous section, the selection of NPs concentration (0.9 wt%) were made to satisfy both cleaning efficiency and economic considerations. In this study, the fluid inlet velocity is varied at both base and 0.9 wt% nanodrilling fluids. The NPs addition and fluid inlet velocity improve fluid carrying capacity for drilled cuttings. Figure 8 represents the impact of fluid velocity on the carrying capacity of the NP-based mud and base mud. An increase in cuttings recovery is observed as the inlet velocity increases for both fluids. However, this increase is more with 0.9 wt% nanodrilling fluids. During a drilling operation when a mud engineer noticed that the hole was not being cleaned of cuttings at a satisfactory rate, the circulation rate and thicken the drilling fluids increased. This justifies why more cuttings recovery with nanofluid. This could be explained mathematically by using Equations (3.1) and (3.2) as well as shown in Figure 7.⁴⁷

$$V_{\text{particle}} = V_{\text{fluid}} - V_{\text{slip}} \quad (3.1)$$

$$V_{\text{slip}} = \frac{138 (\rho_s - \rho_f) d_s^2}{\mu} \quad (3.2)$$

Therefore, more cuttings recovery rate can be obtained by increasing the fluid velocity and viscosity. On the other hand, the increment of the annular fluid velocity results in open hole erosion and uncontrolled losses after fracturing, and the viscosity increment can cause differential sticking problems.⁴⁸ All these parameters should be controlled carefully. An

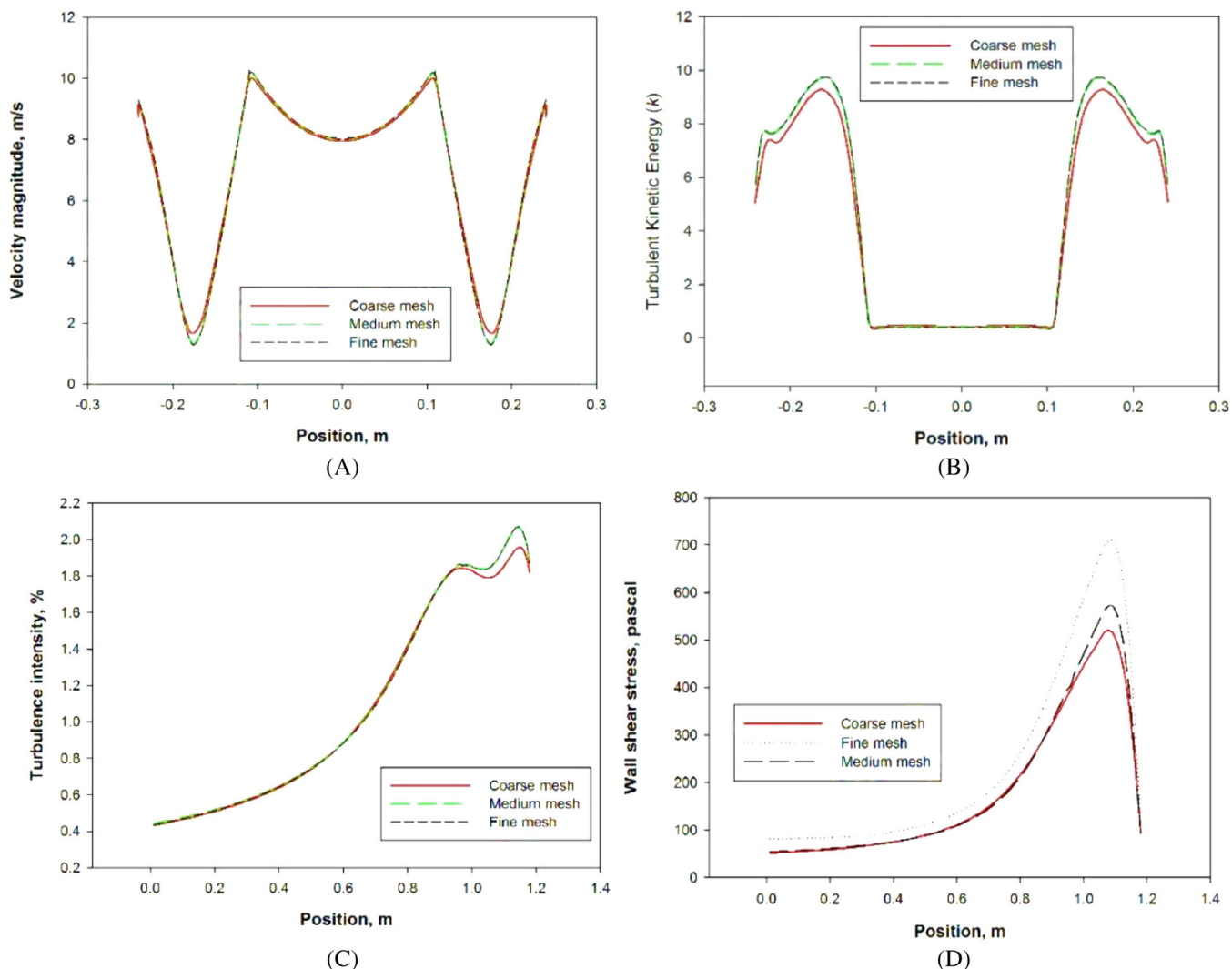


FIGURE 3 A, Velocity magnitude (m/s), B, turbulent kinetic energy (k), C, turbulent dissipation rate (ϵ), and D, wall shear stress. A, B, and C are based on distance along the wellbore diameter ($y = -0.24, 0.24$). D, Graph is calculated based on the distance from top to bottom of the wellbore

important observation shown in Figure 8 is that the cuttings recovery of nanodrilling fluids at low inlet velocity is more than that of the base drilling fluids. (ie, 51% at 0.5 ms⁻¹ for nanofluid and 48% for base fluid). This behavior can help in reducing cuttings deposition when the circulation velocity is not sufficient to overcome the gravitational force.⁴⁹

Drill cuttings in suspension is acted upon by different forces. The diagram below (Figure 9) shows the acting forces on drilled cuttings. The major forces acting on cuttings transport include the drag, buoyancy and gravitational forces. The cuttings characteristics and fluid properties are very important in determining which force is most active and dominates the system. These forces can be grouped into static and hydrodynamic forces. Gravity and buoyancy forces are static forces due to the properties of the particles and its surrounding fluid. Drag is a hydrodynamic force incurred from the fluid flow. Particles start accumulating when the fluid drag is not adequate to enable further motion of the particles. In vertical wells, drag force should surpass gravitational force, which is almost in the opposite direction of the drag force. Otherwise, upwards particle motion will be terminated and particle settling will occur.⁵⁰ Figure 10 demonstrates that the higher in situ concentration of drilled cuttings, the larger the cuttings transport rate. As the height of the cuttings bed becomes more prominent, the fluid can hold more cuttings until attaining the critical carrying capacity. The increasing flow turbulence results in a uniform drag distribution that lifts the cuttings to the surface. These results are consistent with Hussaini and Azar⁵¹ findings who suggested that mud annular velocity decreases in situ cuttings concentration.⁵² However, the mud flow rate needs to be systematically restricted for controlling the pressure drop, pumping cost and wellbore stability.

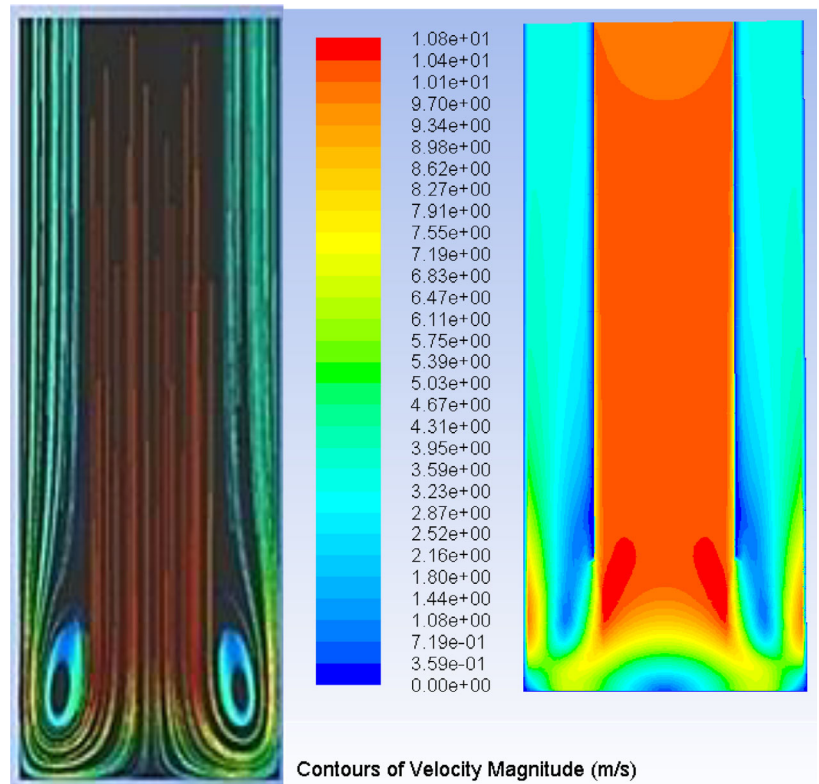


FIGURE 4 (Left) Flow streamline in 2D view. (Right) Velocity magnitude contour

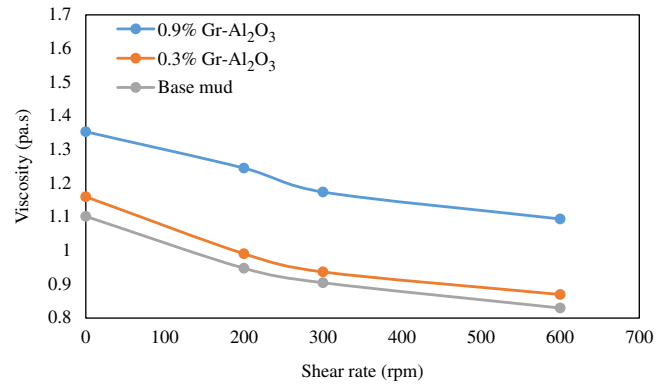


FIGURE 5 Effects of nanoparticles addition on the fluid viscosity

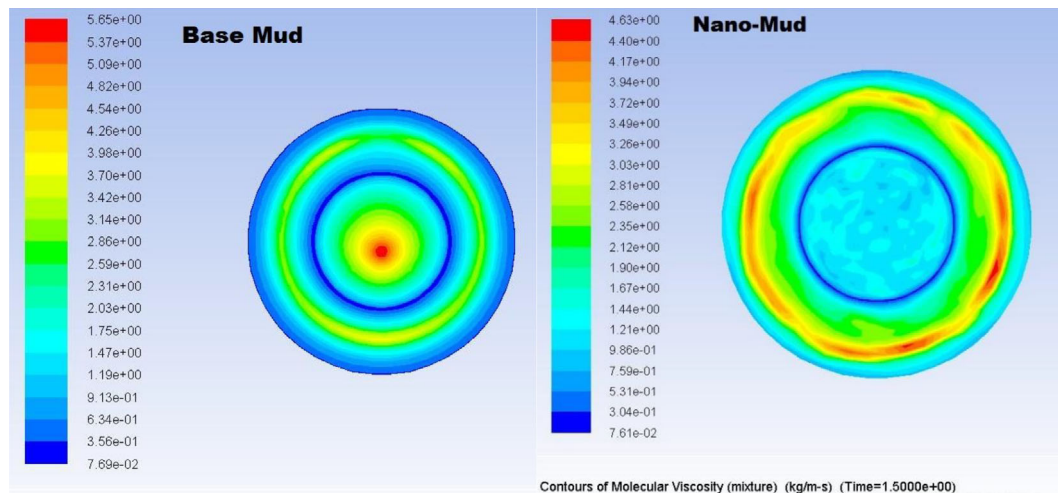


FIGURE 6 Cross-sectional contour of the fluid viscosity for base mud and nano-based mud (100 rpm)

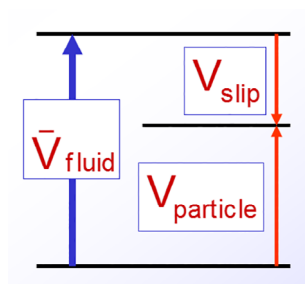


FIGURE 7 Schematic of velocities balance during drilling

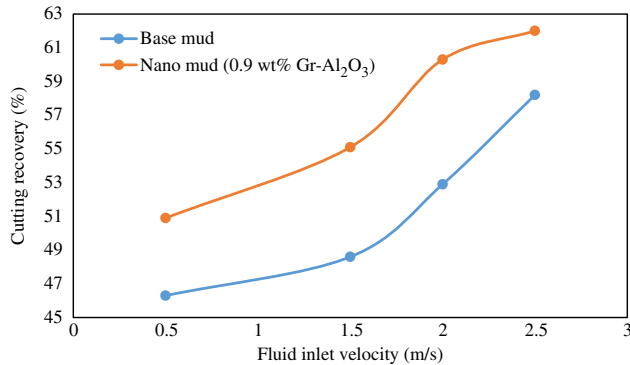
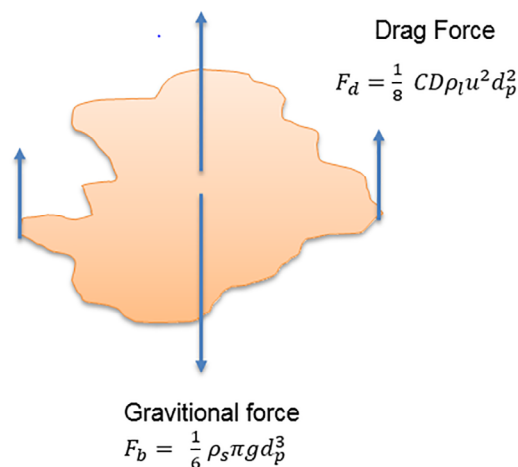


FIGURE 8 Cuttings recovery vs fluid inlet velocity for drill pipe rotation speed of 100 rpm

Buoyancy force

$$F_b = \frac{1}{6} \rho_l \pi g d_p^3$$

FIGURE 9 Forces acting on a drilled cutting



The shape of the cutting's particle can affect the hole cleaning process. Besides the spherical particles, transport of particles with a shape factor of 0.9 and 0.8 were tested at a fixed in situ concentration of 40 wt%. Figure 11 indicates that the particles with higher sphericity are easier to be carried, which is due to its good sliding capability on each other. This also theoretically confirmed with Haider and Levenspiel⁵³ approach for non-spherical particles drag that stated that the shape factor lowers the drag coefficient, hence the resistance to particles transport is more likely to be lower.

The last parameter investigated is cuttings density. The particles with low relative density have better cleaning efficiency. The heavier cuttings tend to settle to the wellbore bottom, as illustrated in Figure 12. The obtained results are confirmed by Li and Wilde⁵⁴ and Zakerian et al.⁵⁵ The authors pointed out that a particle with a higher density is harder to transport through a wellbore. The reason behind that is the gravitational force increase when the density of cuttings particles increases (Figure 9 and Equation 3.2). Increase in cuttings density tends to increase slip velocity, which adversely affects hole cleaning as a result of more cuttings settling. While the opposite occurs when the density of the drilling fluids is increased. The increase in fluid density push buoyancy force to increase and that increase cuttings recovery. An

FIGURE 10 The effects of cuttings in situ concentration on the cuttings recovery for, A, 0.9 wt% Gr-Al₂O₃ nanoparticle mud and B, base mud, at 100 rpm

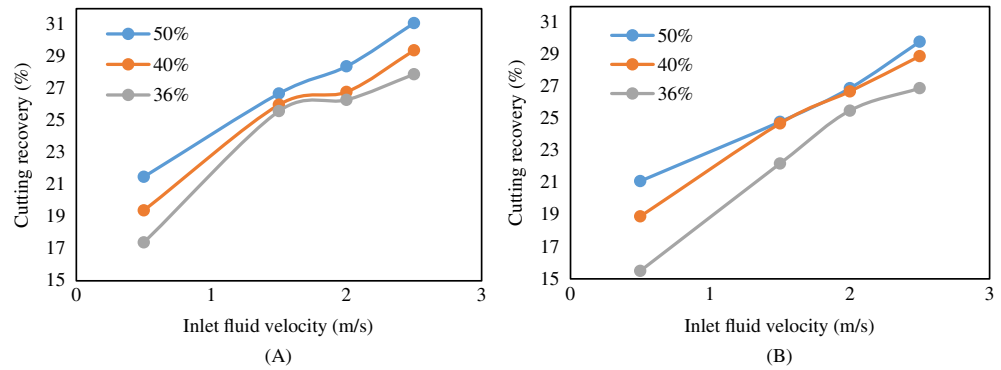


FIGURE 11 The effects of cuttings shape on the cuttings recovery for, A, 0.9 wt% Gr-Al₂O₃ nanoparticle mud and B, base mud, at 100 rpm

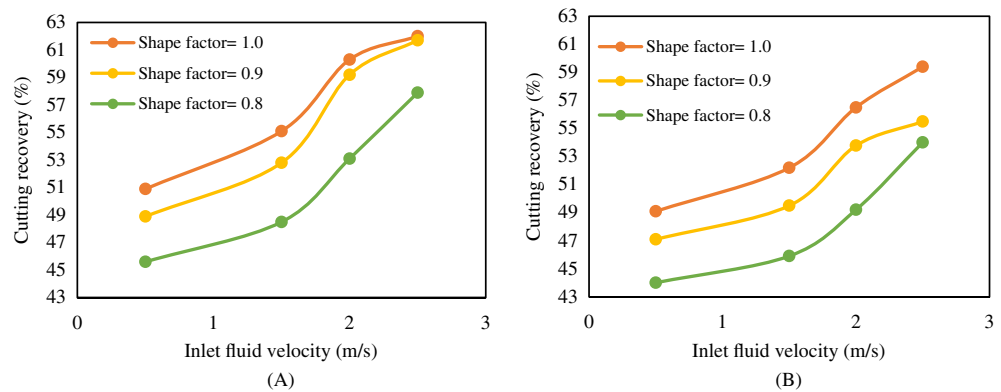
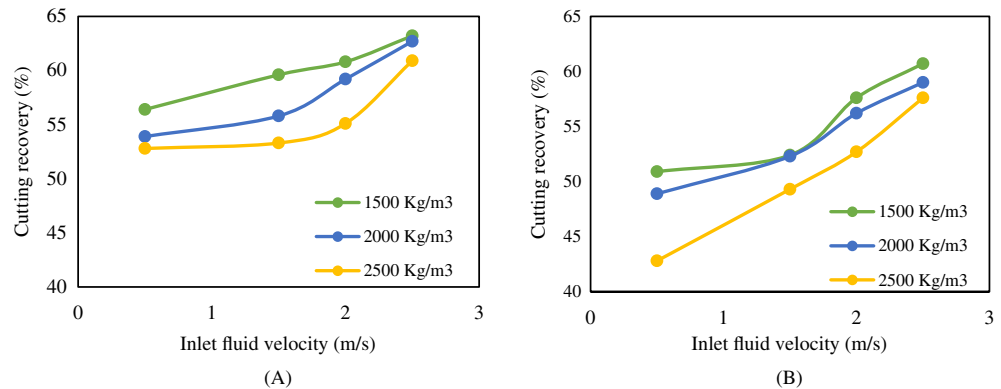


FIGURE 12 The effects of cuttings shape on the cuttings recovery for, A, 0.9 wt% Gr-Al₂O₃ nanoparticle mud and B, base mud, at 100 rpm



important observation shown in Figures 8 and Figures 10, 11, and 12 is the cuttings recovery of drilling fluids can increase with NPs addition. The addition of NPs to water-based mud (WBM) could improve the viscosity, viscoelasticity and thixotropy properties of WBM as well as the ratio of yield point to plastic viscosity. Generally, a drilling fluid with lower plastic viscosity and higher yield point is recommended as the lower plastic viscosity provides turbulence at the drill bit for better hole cleaning and higher yield point ensures enhanced carrying capacity and strong shear thinning behavior.

4 | CONCLUSIONS

The present study numerically examined the performance of cuttings transport process of non-Newtonian NP-based drilling fluids in a vertical non-porous wellbore via ANSYS. The rheological behavior of drilling fluids was characterized by the three-parameter Herschel-Bulkley model. Two categories of suspended particles were used: drilled cuttings and nanomaterials. The interaction between the continuous phase and discrete phases was established by calculating the exchange of drag force, pressure gradient force and lift force according to the two-way coupling regime. The size of NPs was uniform, while cuttings particles size was distributed via the Rosin-Rammler method. To maintain wellbore

conditions, the heat flux from the wellbore wall was considered by including UDF to reflect geothermal gradient impact, which means wall temperature increases with depth.

The present model has successfully predicted some reported facts as follows:

- The flow pattern is turbulent complex and disordered in the bottom of a wellbore.
- Adding NPs with adequate concentration significantly boosts fluid viscosity and carrying capacity.
- Increasing fluid inlet velocity enhances the cleaning performance.
- The cuttings transport process is influenced by cuttings characteristics such as in situ concentration, shape, and density.

CONFLICT OF INTEREST

The authors certify that they have no affiliations with or involvement in any organization or entity with any financial interest (such as honoraria; educational grants; participation in speakers' bureaus; membership, employment, consultancies, stock ownership, or other equity interest; and expert testimony or patent-licensing arrangements), or nonfinancial interest (such as personal or professional relationships, affiliations, knowledge, or beliefs) in the subject matter or materials discussed in this manuscript.

AUTHOR CONTRIBUTIONS

Mortatha Alyasiri: Methodology; supervision; validation; writing-original draft; writing-review and editing. **Amthal Al-Gailani:** Validation. **Dongsheng Wen:** Supervision; writing-review and editing.

NOMENCLATURE

V_q	volume of phase
q	phases
v	velocity
p	pressure
g	acceleration gravity constant
F_D	drag force
F_b	Buoyancy force
F_g	gravitational force
K	consistency index or thermal conductivity
n	power law index
E_a	activation energy
T	temperature
Q	conductive heat transfer
V_{slip}	slip velocity

Greek symbols

α_q	phasic volume fraction
ρ_q	phase density
τ	stress tensor
μ_t	turbulent viscosity
ε	turbulent dissipation rate
η	dynamic viscosity
γ	shear rate
τ_o	yield stress threshold
γ_c	critical shear rate
ρ_s	density of cuttings
ρ_f	density of drilling fluid
μ	viscosity

ORCID

Mortatha Al-Yasiri  <https://orcid.org/0000-0002-7180-5493>

Amthal Al-Gailani  <https://orcid.org/0000-0001-9290-0636>

REFERENCES

1. Al-Yasiri M, Awad A, Pervaiz S, Wen D. Influence of silica nanoparticles on the functionality of water-based drilling fluids. *J Petrol Sci Eng.* 2019;179:504-512.
2. Rafati R, Smith SR, Haddad AS, Novara R, Hamidi H. Effect of nanoparticles on the modifications of drilling fluids properties: a review of recent advances. *J Petrol Sci Eng.* 2018;161:61-76.
3. Al Ruqeishi MS, Al Salmi Y, Mohiuddin T. Nanoparticles as Drilling Fluids Rheological Properties Modifiers. *Progress in Petrochemical Science.* 2018;1:97-103.
4. Al-Yasiri M, Wen D. Gr-Al₂O₃ nanoparticles based multi-functional drilling fluid. *Ind Eng Chem Res.* 2019;58:10084-10091.
5. Dhiman P, Cheng Y, Zhang Y, Patil S. Experimental investigation of the influence of nanoparticles on water-based mud. *Appl Nanosci.* 2018;8:511-526.
6. Song K, Wu Q, Li M-C, et al. Performance of low solid bentonite drilling fluids modified by cellulose nanoparticles. *J Nat Gas Sci Eng.* 2016;34:1403-1411.
7. Abdo J, Danish M. *Nanoparticles: Promising Solution to Overcome Stern Drilling Problems.* Anaheim, CA: Nanotech Conference and Exhibition; 2010:6-8.
8. Agarwal S, Tran P, Soong Y, Martello D, Gupta K. *Flow Behavior of Nanoparticle Stabilized Drilling Fluids and Effect of High Temperature Aging.* Houston, TX: AADE National Technical Conference and Exhibition; 2011:12-14.
9. Barry MM, Jung Y, Lee J-K, Phuoc TX, Chyu MK. Fluid filtration and rheological properties of nanoparticle additive and intercalated clay hybrid bentonite drilling fluids. *J Petrol Sci Eng.* 2015;127:338-346.
10. Ghasemi N, Mirzaee M, Aghayari R, Maddah H. Investigating created properties of nanoparticles based drilling mud. *Heat Mass Transf.* 2018;54:1381-1393.
11. Jahns C. *Friction Reduction by Using Nano-Fluids in Drilling.* Master's thesis, Institutt for petroleumsteknologi og anvendt geofysikk; 2014.
12. Nasser J, Jesil A, Mohiuddin T, Al Ruqeshi M, Devi G, Mohataram S. Experimental investigation of drilling fluid performance as nanoparticles. *World J Nano Sci Eng.* 2013;2013:57-61.
13. Sayyadnejad M, Ghaffarian H, Saeidi M. Removal of hydrogen sulfide by zinc oxide nanoparticles in drilling fluid. *Int J Environ Sci Technol.* 2008;5:565-569.
14. Vryzas Z, Mahmoud O, Nasr-el-Din HA, Kelessidis VC. Development and testing of novel drilling fluids using Fe₂O₃ and SiO₂ nanoparticles for enhanced drilling operations. *International Petroleum Technology Conference.* 6-9 December, Doha, Qatar; 2015.
15. William JKM, Ponmani S, Samuel R, Nagarajan R, Sangwai JS. Effect of CuO and ZnO nanofluids in xanthan gum on thermal, electrical and high pressure rheology of water-based drilling fluids. *J Petrol Sci Eng.* 2014;117:15-27.
16. Versteeg HK, Malalasekera W. *An Introduction to Computational Fluid Dynamics: The Finite Volume Method.* Harlow, England: Pearson Education; 2007.
17. Al-Yasiri MS, Al-Sallami WT. How the drilling fluids can be made more efficient by using nanomaterials. *Am J Nano Res Appl.* 2015;3:41-45.
18. Aftab A, Ismail AR, Ibupoto ZH, Akeiber H, Malghani MGK. Nanoparticles based drilling muds a solution to drill elevated temperature wells: a review. *Renew Sustain Energy Rev.* 2017;76:1301-1313.
19. Mao H, Qiu Z, Shen Z, Huang W. Hydrophobic associated polymer based silica nanoparticles composite with core-shell structure as a filtrate reducer for drilling fluid at ultra-high temperature. *J Petrol Sci Eng.* 2015;129:1-14.
20. Huang X, Lv K, Sun J, et al. Enhancement of thermal stability of drilling fluid using laponite nanoparticles under extreme temperature conditions. *Mater Lett.* 2019;248:146-149.
21. Wang K, Jiang G, Liu F, Yang L, Ni X, Wang J. Magnesium aluminum silicate nanoparticles as a high-performance rheological modifier in water-based drilling fluids. *Appl Clay Sci.* 2018;161:427-435.
22. Saboori R, Sabbaghi S, Barahoei M, Sahooli M. Improvement of thermal conductivity properties of drilling fluid by CuO nanofluid. *Transp Phenom Nano Micro Scales.* 2017;5:97-101.
23. Bilgesu H, Ali M, Aminian K, Ameri S. Computational fluid dynamics (CFD) as a tool to study cutting transport in wellbores. *SPE Eastern Regional Meeting.* 23-26 October, Lexington, Kentucky: Society of Petroleum Engineers; 2002.
24. Kabir MA, Gamwo IK. Filter cake formation on the vertical well at high temperature and high pressure: computational fluid dynamics modeling and simulations. *J Petrol Gas Eng.* 2011;7:146-164.
25. Chen X-Z, Shi D-P, Gao X, Luo Z-H. A fundamental CFD study of the gas-solid flow field in fluidized bed polymerization reactors. *Powder Technol.* 2011;205:276-288.
26. Zhang N, Lu B, Wang W, Li J. 3D CFD simulation of hydrodynamics of a 150 MW_e circulating fluidized bed boiler. *Chem Eng J.* 2010;162:821-828.
27. Akhshik S, Behzad M, Rajabi M. CFD-DEM model for simulation of non-spherical particles in hole cleaning process. *Part Sci Technol.* 2015;33:472-481.
28. Tsuji Y, Kawaguchi T, Tanaka T. Discrete particle simulation of two-dimensional fluidized bed. *Powder Technol.* 1993;77:79-87.
29. Xu B, Yu A. Numerical simulation of the gas-solid flow in a fluidized bed by combining discrete particle method with computational fluid dynamics. *Chem Eng Sci.* 1997;52:2785-2809.
30. Xu M, Chen F, Liu X, Ge W, Li J. Discrete particle simulation of gas-solid two-phase flows with multi-scale CPU-GPU hybrid computation. *Chem Eng J.* 2012;207:746-757.
31. Mme U, Skalle P. CFD calculations of cuttings transport through drilling annuli at various angles. *Int J Petrol Sci Technol.* 2012;6:129-141.
32. Popoff B, Braun M. A Lagrangian approach to dense particulate flows. *International Conference on Multiphase Flow, Leipzig, Germany;* 2007.

33. Cloete S, Johansen S, Braun M, Popoff B, Amini S. Evaluation of a Lagrangian discrete phase modeling approach for resolving cluster formation in CFB risers. *7th International Conference on Multiphase Flow*, Tampa, FL; 2010.
34. Alyasiri M, Antony J, Wen D. *Enhancement of Drilling Fluid Rheology by Nanoparticles*. Malmö, Sweden: Nordic Rheology Society; 2017.
35. Drew DA. Mathematical modeling of two-phase flow. *Annu Rev Fluid Mech*. 1983;15:261-291.
36. FLUENT. *15—Theory Guide*. Canonsburg, PA: ANSYS; 2015.
37. Launder BE, Spalding DB. *Lectures in Mathematical Models of Turbulence*. London; New York: Academic Press; 1972.
38. Mei R. An approximate expression for the shear lift force on a spherical particle at finite Reynolds number. *Int J Multiph Flow*. 1992;18:145-147.
39. Oesterle B, Dinh TB. Experiments on the lift of a spinning sphere in a range of intermediate Reynolds numbers. *Exp Fluids*. 1998;25:16-22.
40. Saffman P. The lift on a small sphere in a slow shear flow. *J Fluid Mech*. 1965;22:385-400.
41. Fisher K, Wakeman R, Chiu T, Meuric O. Numerical modelling of cake formation and fluid loss from non-Newtonian muds during drilling using eccentric/concentric drill strings with/without rotation. *Chem Eng Res Des*. 2000;78:707-714.
42. Huilgol RR, You Z. Application of the augmented Lagrangian method to steady pipe flows of Bingham, Casson and Herschel-Bulkley fluids. *J Non-Newtonian Fluid Mech*. 2005;128:126-143.
43. Samsuri A, Hamzah A. Water based mud lifting capacity improvement by multiwall carbon nanotubes additive. *J Petrol Gas Eng*. 2011;5:99-107.
44. Baker TJ. Mesh generation: art or science? *Prog Aerosp Sci*. 2005;41:29-63.
45. Holland F, Bragg R. *Fluid Flow for Chemical and Process Engineers*. England: Butterworth-Heinemann; 1995.
46. Vryzas Z, Kelessidis VC. Nano-based drilling fluids: a review. *Energies*. 2017;10:540.
47. Shearer SA, Hudson JR. Fluid mechanics: stokes' law and viscosity. *Meas Lab*. 2008;3:1-7.
48. Sayindla S, Lund B, Ytrehus JD, Saasen A. CFD modelling of observed cuttings transport in oil-based and water-based drilling fluids. *SPE/IADC Drilling Conference and Exhibition*. 14-16 March, The Hague, The Netherlands: Society of Petroleum Engineers; 2017.
49. Epelle EI, Gerogiorgis DI. A multiparametric CFD analysis of multiphase annular flows for oil and gas drilling applications. *Comput Chem Eng*. 2017;106:645-661.
50. Morsi S, Alexander A. An investigation of particle trajectories in two-phase flow systems. *J Fluid Mech*. 1972;55:193-208.
51. Hussaini SM, Azar JJ. Experimental study of drilled cuttings transport using common drilling muds. *Soc Petrol Eng J*. 1983;23:11-20.
52. Dewangan SK, Sinha SL. Exploring the hole cleaning parameters of horizontal wellbore using two-phase Eulerian CFD approach. *J Comput Multiph Flows*. 2016;8:15-39.
53. Haider A, Levenspiel O. Drag coefficient and terminal velocity of spherical and nonspherical particles. *Powder Technol*. 1989;58:63-70.
54. Li J, Wilde G. Effect of particle density and size on solids transport and hole cleaning with coiled tubing. *SPE/ICoTA Coiled Tubing Conference and Exhibition*. 12-13 April, The Woodlands, Texas: Society of Petroleum Engineers; 2005.
55. Zakerian A, Sarafraz S, Tabzar A, Hemmati N, Shadizadeh SR. Numerical modeling and simulation of drilling cutting transport in horizontal wells. *J Petrol Explor Prod Technol*. 2018;8:455-474.

How to cite this article: Al-Yasiri M, Al-Gailani A, Wen D. Numerical study of cuttings transport of nanoparticle-based drilling fluid. *Engineering Reports*. 2020;2:e12154. <https://doi.org/10.1002/eng2.12154>